PAPER

Check for updates

Autonomous robotic experimentation system for powder X-ray diffraction†

Yuto Yotsumoto, [ID] Yusaku Nakajima, [ID] Ryusei Takamoto, Yasuo Takeichi [ID] and Kanta Ono [ID] *

The automation of materials research is essential for accelerating scientific discovery. Powder X-ray diffraction (PXRD) plays a crucial role in analyzing crystal structures and quantifying phase compositions in materials science. However, current methods face challenges in reproducibility and efficiency. To address these issues, we developed an autonomous robotic experimentation (ARE) system for PXRD that integrates the entire process from sample preparation to data analysis. This system combines a robotic arm for precise sample preparation with machine learning-based techniques for automated data analysis. Our approach consistently produced high-quality samples with reduced background noise, achieving accuracy comparable to manual preparation techniques. We also investigated the relationship between sample quantity and analysis accuracy, demonstrating the system's ability to obtain reliable results with significantly reduced sample amounts. This work advances laboratory automation capabilities and contributes to the development of autonomous materials discovery and optimization processes. By addressing key challenges in PXRD automation, our research enables more efficient and reproducible materials characterization methodologies.

1 Introduction

Laboratory automation using robots to perform repetitive tasks reproducibly has become increasingly important in materials research and development.[1–12] Among various experimental techniques, powder X-ray diffraction (PXRD) provides crucial data in materials science, offering diverse information such as crystal structure determination,[13–15] phase identification and quantification,[16] and crystal polymorph characterization.[14,17–21] While autonomous workflows for PXRD have been proposed,[10,12,22] some approaches result in high background intensity at low angles due to sample preparation methods, which can hinder accurate quantitative analysis in this region. This limitation poses a challenge for effectively analyzing certain materials with important structural features in the low-angle region. Low-angle patterns are essential for characterizing a wide range of materials, including organic compounds[23,24] and lead halide perovskites.[25–28] For example, lead halide perovskites have emerged as promising materials for optoelectronic devices, and low-angle peaks in the range of 10 to 20 degrees are used to identify the reactants and products and to verify the occurrence of the reactions.[25,28] Therefore, the reduction of background noise, particularly at low angles, is

essential for expanding the applicability of automated PXRD systems to a broader range of materials.

High-throughput experimental studies involving the creation of large sample libraries and their rapid characterization using automated or parallelized techniques have become increasingly important in material discovery and optimization.[29–31]

To address these challenges and advance materials science, we have developed an autonomous robotic experimentation (ARE) system for PXRD that integrates all processes of the PXRD experiments. The ARE system combines a robotic arm for precise powder sample preparation with machine learning techniques for automated XRD data analysis, enabling a highly automated workflow from sample handling to result interpretation. This system achieves high-precision measurements and analysis using significantly smaller sample quantities and implements automation without requiring extensive modifications to existing PXRD equipment. As a result, the ARE system facilitates easier adoption in research laboratories. It enhances the consistency of sample preparation processes and contributes to improved reproducibility of measurement results. These features enable efficient high-throughput materials research. Furthermore, by combining this system with robot-assisted material synthesis and materials informatics-based design, a powerful data-driven approach to accelerate material discovery and optimization becomes possible.

In summary, our contributions are as follows:

Department of Applied Physics, Osaka University, Osaka, Japan. E-mail: yuto_yotsumoto@ap.eng.osaka-u.ac.jp; ono@ap.eng.osaka-u.ac.jp

(1) We developed an autonomous experimentation system for PXRD that integrates the entire workflow from sample preparation to data analysis; compared to manual methods, our system achieved high precision and reliability in sample preparation.

(2) We demonstrated the ability of precise robotic sample preparation to obtain low-background patterns, especially at low angles.

(3) We investigated the effect of the sample quantity on the accuracy and consistency of quantitative analysis using our autonomous system; thus, reliable results could be obtained with significantly reduced sample amounts than those used in manual preparation methods.

(4) We validated the autonomous system with different mixture ratios and showed its accuracy in quantifying phase compositions.

The remainder of this paper is organized as follows. In Section 2, the development of an autonomous PXRD system that incorporates a robotic arm for sample handling and preparation is presented. In Section 3, a detailed description of the experimental workflow of PXRD is provided, and the key steps involved in the process are outlined. In Section 4, the automation of quantitative XRD data analysis is discussed. In Section 5, the results obtained from the autonomous PXRD system are shown, and a detailed discussion of the implications of these findings for material characterization and discovery is provided. The section also addresses the system's current limitations and future prospects. Finally, in Section 6, the paper is concluded, and future research directions are proposed.

2 Development of an autonomous PXRD system

Fig. 1 shows the workflow and setup of the ARE system for PXRD.

The main components of the ARE system are as follows:

(1) The 6-axis robotic arm (DENSO, COBOTTA) with a multi-functional end effector for sample preparation and handling (Fig. 2a).

(2) A detachable protective cover made of paper, used to protect the soft gel attachment on the robotic arm's end effector from contamination. The robotic arm's automated movements enable the cover to be attached before sample preparation and detached after use. This ensures a clean environment for each sample without human intervention.

(3) An XRD instrument (Rigaku, MiniFlex 600-C) is equipped with a single-axis actuator to control the door. The single-axis actuator enables the automatic opening and closing of the doors of the XRD instrument.

(4) A sample holder featuring a frosted glass surface and embedded magnets (Fig. 2b). This design supports the powder sample, facilitates automated handling, and contributes to high-quality XRD measurements.

(5) A drawer-based sample hotel serves as a storage unit for multiple sample holders and has 20 tiers to accommodate up to 40 samples in total.

(6) A sample preparation station is used for processing powder samples into an optimized form for XRD analysis; this features an integrated pull-out funnel for precise centering of the powder within the holder.

The end effector of the robotic arm is a key component of our system and shown in detail in Fig. 2a. The end effector was fabricated using a 3D printer (Formlabs, Form 3+), which enabled the precise customization of its design. As illustrated, the end effector integrates three attachments: a claw for drawer manipulation, a metal plate for magnetic coupling with the sample holder, and a soft gel for surface flattening. This design allows for sample preparation, loading, and unloading, as well as the opening and closing of drawers, without changing attachments. The end effector includes a soft gel for sample surface flattening, protected by a cover that is automatically attached before and detached after sample preparation by the robotic arm's movements, preventing cross-contamination between samples. Due to this integrated design, the efficiency and autonomy of the system is improved. The use of soft gel attachment on the end effector for sample preparation is likely a key factor to attain low-background patterns. The gel enables the gentle and uniform pressing of the powder sample; this results in a smooth and even surface that minimizes the background noise.

To further optimize the automation process, a single-axis actuator is incorporated to control the doors of the XRD instrument. This eliminates the need for the robotic arm to perform the door opening and closing tasks, simplifies the overall workflow and reduces the risk of interference between the arm and the instrument.

Fig. 2b shows our sample holder, which is an essential component of the system. The sample holder's central area is made of frosted glass, which serves two purposes: (1) supports the powder sample and prevents the sample from falling, and (2) aids in the reduction of the background noise in the XRD measurements. The frosted surface effectively balances the sample retention with minimal contribution to background intensity; this aspect is particularly useful for the accurate analysis in the low-angle regions. The outer frame of the sample holder contains embedded magnets for secure attachment to the metal plate of the end effector during transfer and manipulation. This design enables the stable and precise sample handling throughout the automated process, from preparation to measurement, and preserves the sample integrity and XRD data quality.

By integrating these components, the ARE system automates much of the XRD sample preparation and measurement process. This automation aims to reduce human errors, enhance consistency in sample preparation, and potentially increase sample throughput.

Due to its modular design, the autonomous PXRD system can be readily adapted to other analytical methods and sample synthesis processes. The robotic arm, sample hotel, and other components of the system, such as the sample preparation station and the control software, can be easily integrated with other characterization techniques. For example, the sample preparation station can be modified to accommodate specific
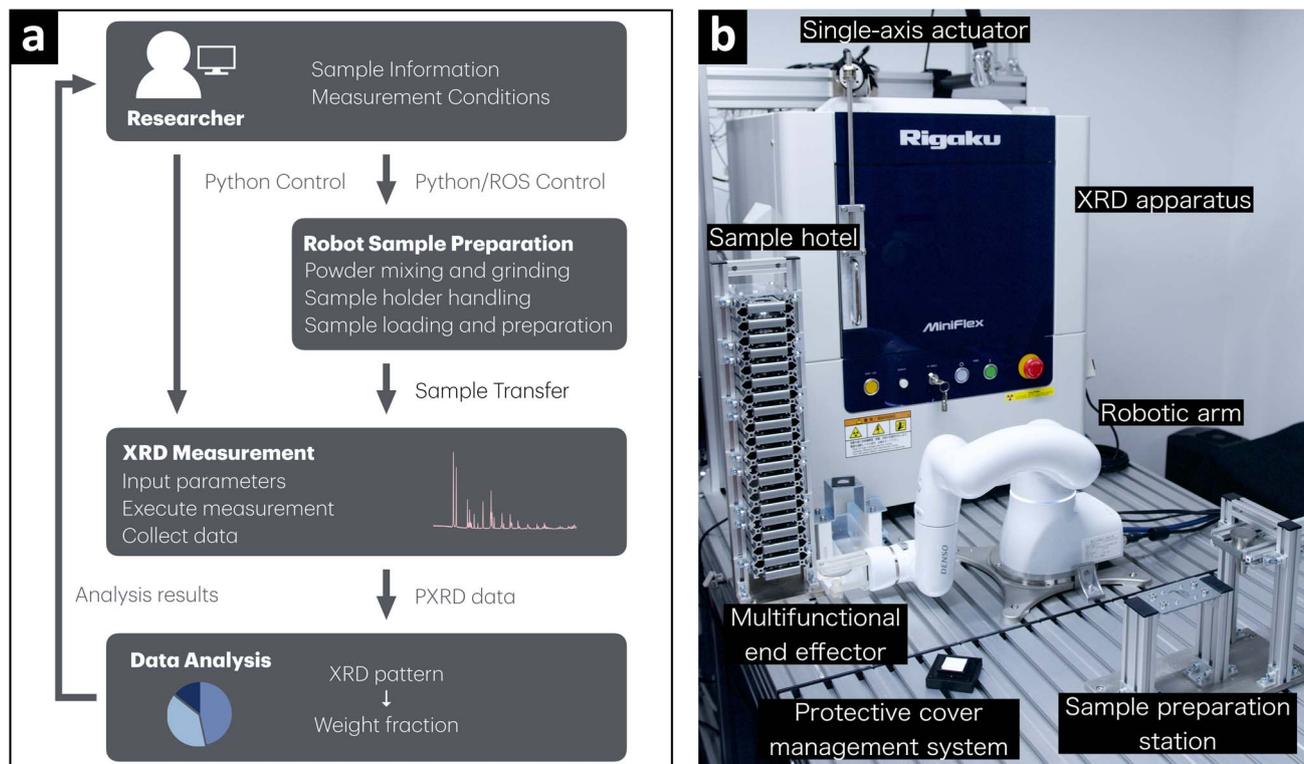
Fig. 1 Autonomous PXRD system overview. (a) Schematic representation of the autonomous PXRD experimental workflow. The researcher initiates the measurement process by sending commands to the control PC. The robotic arm prepares the sample and loads it into the XRD instrument; then, the measurement is performed. The data are then automatically analyzed, and the results are returned to the researcher; this process completes the experimental loop. (b) Key components of the autonomous PXRD system setup; the setup includes a robotic arm, sample preparation station, sample hotel, and an XRD instrument and enables a fully automated and efficient PXRD experiment.
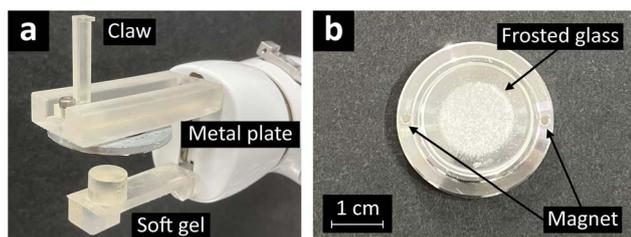

Fig. 2 Close-up view of the key components in the ARE system. (a) Multifunctional end effector consisting of three attachments: a claw for opening and closing the drawers, a metal plate for magnetically transporting the sample holder, and a soft gel for gently flattening the powder sample surface. (b) Sample holder featuring a central area made of frosted glass, which provides a surface that prevents the powder sample from falling through. The magnets are embedded in the outer frame of the sample holder; thus, for the sample holder can be securely attached to the metal plate of the end effector during transfer and to the preparation stage during manipulation.

requirements for techniques such as Raman spectroscopy, while the control software can be adapted to coordinate the operation of multiple instruments; thus, multimodal analysis of the samples is possible. Furthermore, the automated workflow can be extended to include additional sample synthesis steps, such as weighing and mixing of the precursor materials; this creates a fully autonomous material discovery pipeline. Due to

its flexibility and adaptability, the autonomous PXRD system is a valuable tool for accelerating material research and discovery across a wide range of applications.

3 Detailed workflow of the autonomous PXRD system

The autonomous PXRD system operates according to a workflow that minimizes human intervention and significantly increases automation. Fig. 3 illustrates the key processes performed by the robotic arm in our autonomous PXRD system. The detailed steps in the workflow are as follows:

Step 1: the researcher sends a command to the control PC specifying the sample information and measurement parameters.

Step 2: the control PC processes the command and sends instructions to the robotic arm and the XRD instrument.

Step 3: the robotic arm (Universal Robots, UR5e) mixes and grinds the powder sample to ensure homogeneity, as described in our previous work[32,33] (Fig. 3a).

Step 4: the robotic arm retrieves the specified sample holder from the sample hotel and transfers it to the sample preparation station (Fig. 3b).

Step 5: the ground powder is filled into the sample holder placed at the sample preparation station. While the robotic arm
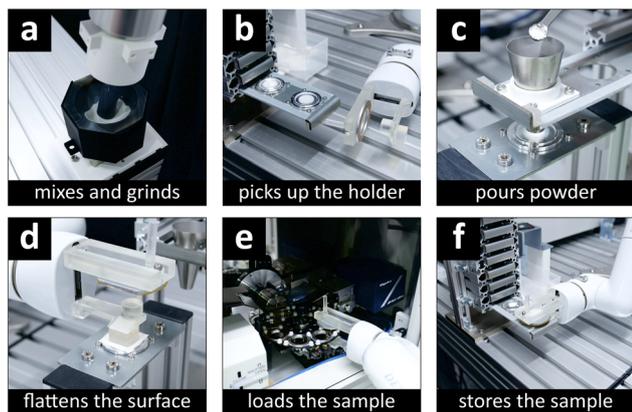
Fig. 3 Key processes performed by the robotic arm in the autonomous PXRD system. (a) The robotic arm mixes and grinds the powder sample to ensure homogeneity and appropriate particle size. (b) The robotic arm picks up the sample holder using a multifunctional end effector. (c) In this study, the prepared powder sample is manually poured into the sample holder due to the need to measure the amount of powder used. To note, the robotic arm is technically able to perform this step; however, in the current experiment, this was manually performed. (d) Using a soft gel attachment on the end effector, the robotic arm gently flattens the surface of the powders to ensure a smooth and even surface for the XRD measurement. (e) The robotic arm loads the prepared sample into the XRD instrument for measurement. (f) After the measurement is completed, the robotic arm stores the sample in the designated position of the sample hotel.

is technically capable of performing this step autonomously, in this study, it was done manually to measure the precise amount of powder used (Fig. 3c).

Step 6: the robotic arm uses soft gel attached to the end effector to gently flatten the surface of the powder sample (Fig. 3d).

Step 7: the XRD instrument automatically opens its door using a single-axis actuator, and the robotic arm loads the prepared sample into the instrument (Fig. 3e).

Step 8: the XRD instrument closes its door, and the measurement software is automatically controlled to start the measurement according to the specified parameters.

Step 9: after the measurement is complete, the XRD instrument sends the raw data (XRD pattern) to a workstation, and the robotic arm retrieves the sample from the XRD instrument and returns it to the sample hotel (Fig. 3f).

Step 10: the workstation automatically analyzes the XRD pattern using an automated Rietveld analysis method; the pattern is converted into weight fractions of its constituent phases.

Step 11: the analyzed results are sent back to the researcher, and the automated PXRD experiment is complete.

The automation of the XRD measurement software is achieved using PyAutoGUI, a Python library that controls mouse and keyboard inputs. This approach allows for the operation of proprietary software without direct API access, enabling the seamless integration of the XRD instrument into the autonomous workflow.

4 Automation of quantitative XRD data analysis

Automating the analysis of measurement data is a crucial component of a fully closed autonomous measurement workflow. While our developed ARE system integrates all processes from sample preparation to data acquisition, automating data analysis is necessary to achieve self-contained PXRD experiments. In PXRD analysis, the Rietveld method is widely used, enabling quantitative analysis of phase composition, lattice constants, and other structural parameters. However, Rietveld refinement is a time-consuming and labor-intensive task, requiring the optimization of dozens of parameters related to crystal structure, instrumentation, line shape, and background. Traditional manual parameter adjustment requires significant time and effort, even for skilled experts, and faces challenges in reproducibility and consistency of results.

To address these challenges, we previously developed an automated Rietveld refinement method called Blackbox Optimization Rietveld (BBO-Rietveld).[34] BBO-Rietveld treats parameter optimization in Rietveld refinement as a blackbox optimization problem, utilizing Bayesian optimization, specifically the Tree-structured Parzen Estimator (TPE) algorithm, to efficiently explore the high-dimensional parameter space. Conventional Rietveld refinement requires optimizing multiple parameters while considering their interactions and physical constraints, a process that heavily relies on the judgment of experienced experts. This process is not merely random parameter optimization but rather an exploration of physically meaningful structural models. In contrast, BBO-Rietveld adopts an approach focused on minimizing the weighted profile R-factor (R_{wp}), achieving efficient exploration without relying on expert heuristics. This method can obtain highly reproducible results that do not depend on the operator's experience. Furthermore, by systematically exploring a wide parameter space, it has the potential to discover optimal solutions that might have been overlooked by conventional methods. However, BBO-Rietveld also has its challenges. The most critical point is that, being an essentially statistical approach, it may propose solutions that are physically or chemically meaningless. For example, models with unrealistically short interatomic distances or structurally impossible configurations might be proposed as solutions if they result in a low R_{wp}. Therefore, experts need to carefully evaluate the physical validity of the obtained results.

Furthermore, the BBO-Rietveld method can address the issue of preferred orientation, which is a common problem in Bragg–Brentano geometry. By including orientation parameters in the optimization process, it can automatically adjust for the effects of preferred orientation that may occur in compressed samples. However, in cases of severe preferred orientation, expert interpretation of the results and additional sample preparation techniques may be necessary.

BBO-Rietveld integrates the Python-based Rietveld refinement software GSAS-II[35] with the hyperparameter optimization framework Optuna.[36] We have incorporated this system into our

autonomous PXRD setup, enabling automated data analysis and enhancing the efficiency of crystal structure determination. Moreover, BBO-Rietveld's computational efficiency can be further improved through parallelization; in our previous work, we demonstrated the ability to complete 200 refinement trials within one hour on a standard workstation.[34]

When using the BBO-Rietveld method, it is necessary to input crystal structure information of potential substances in the sample beforehand. Typically, this information is obtained from crystallographic databases and used as initial structural models. The selection of initial structural models is a critical step that requires careful consideration by experts based on the sample's chemical composition and expected phases. Looking ahead, we aim to develop systems that can automatically generate initial structural models and apply to a wider range of unknown materials by integrating methods such as deep learning. For example, combining recently proposed deep neural networks like CrystalNet[37] with BBO-Rietveld could lead to the construction of a more comprehensive automated analysis pipeline. However, these methods are still in their early stages and require further validation for application to complex real-world systems.

The automation of measurement data analysis using BBO-Rietveld has the potential to enhance the efficiency of materials science research. This method can reduce human bias and variability, thereby improving the reproducibility and consistency of analyses. However, while BBO-Rietveld is effective for analyzing substances with known crystal structures, it faces limitations when dealing with unknown structures or complex multiphase systems. For novel materials or intricate systems, expert verification and interpretation of results remain indispensable. Deep knowledge of crystallography and materials science continues to be crucial for selecting initial structural models, evaluating the physical validity of obtained results, and interpreting the final structural models. Moreover, PXRD data often presents a uniqueness problem, where different structural models may exhibit similarly good fits. To address this issue in complex samples, complementary techniques such as spectroscopy, neutron diffraction, or simulations may be necessary.

Therefore, automated systems including BBO-Rietveld should be positioned as tools to support expert judgment and improve the efficiency of routine analyses for known materials, rather than as replacements for human expertise in crystallography and materials science. These systems aim to assist experts in focusing on more complex and creative problem-solving tasks.

5   Results and discussion

In this study, we conducted three experiments to evaluate the performance and capabilities of the autonomous PXRD system. All XRD measurements were performed under the following conditions: Cu Kα radiation ($\lambda = 1.5419$ Å), voltage of 40 kV, current of 15 mA, scan range of $10°–120°$ 2θ, step size of $0.01°$, scan speed of $4°$ min^{-1}, and sample spin rate of 80 rpm. The incident beam was conditioned using a 5 mm incident slit and

a $1.25°$ divergence slit to control and reduce the irradiated area on the sample surface.

The first experiment, described in Section 5.1, focused on assessing the precision of the robotic arm in sample preparation and its impact on the accuracy of quantitative XRD analysis. The goal was to determine whether the automated system could achieve results comparable to or better than those of the manual sample preparation methods in terms of reproducibility, consistency, and reliability.

The second experiment, detailed in Section 5.2, investigated the effect of the sample quantity on the accuracy and precision of the quantitative XRD analysis. By preparing samples with varying amounts of material using the robotic arm, we aimed to identify the minimum sample quantity needed to obtain reliable anatase content results with a target standard deviation (SD) of less than 1% for the replicate measurements.

Finally, the third experiment, presented in Section 5.3, validated the autonomous system's performance using samples with different mixture ratios of anatase and rutile TiO$_2$. The purpose of this experiment was to demonstrate the system's accuracy in quantifying the phase compositions across a range of sample compositions; this aspect is essential for high-throughput material discovery and optimization.

Through these three experiments, we aimed to comprehensively evaluate the capabilities, limitations, and potential of the autonomous PXRD system for advancing material research and accelerating the discovery of new materials with desirable properties.

5.1   Powder sample preparation by the robotic arm

We evaluated an autonomous PXRD system to investigate the precision of robotic arms in sample preparation and its impact on the accuracy of the quantitative XRD analysis. Our objective was to assess whether an autonomous PXRD system using a robotic arm could enhance the reproducibility, consistency, efficiency, and accuracy of the PXRD sample preparation. We hypothesized that the robotic arm could reduce human error, increase throughput, standardize procedures, and ultimately match or even surpass the accuracy and consistency of the manual sample preparation methods.

We used a robotic arm to prepare samples containing precise quantities of titanium dioxide (TiO$_2$) in its anatase and rutile phases. Fig. 4 shows the samples prepared by manual operation
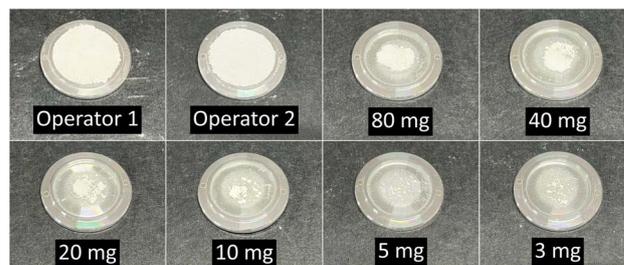

Fig. 4 Photographs of the TiO$_2$ samples prepared by manual operation and the robotic arm in different quantities.

and the robotic arm. The anatase reagent (Kojundo Chemical Laboratory, 99% purity) did not contain any detectable rutile impurities; however, the rutile reagent (Kojundo Chemical Laboratory, 99.99% purity, 2 μm particle size, >90% reutilization rate) contained approximately 2.8% anatase as an impurity. To determine the impurity levels, samples containing only the individual reagents were prepared and analyzed using the BBO-Rietveld method prior to the main experiment. Equal amounts of the two reagents were mixed; this resulted in samples with anatase and rutile weight fractions of approximately 51.4% and 48.6%, respectively. Each sample prepared by the robotic arm weighed 80.0 mg, while samples prepared by human operators weighed approximately 300 mg. To ensure consistency, the robotic arm's repeatability was evaluated across multiple experiments. The resulting data were analyzed *via* the BBO-Rietveld method.

Fig. 5 shows a comparison of the XRD patterns and Rietveld refinement results for the samples prepared by the robotic arm and manual operation. The good agreement between the measured and calculated patterns, along with the small residuals, demonstrates the high quality of the samples prepared by both methods. The robotic arm-prepared samples show low background intensity at low angles, addressing a common challenge in automated sample preparation methods. This achievement can be attributed to the robotic arm's precise control in Step 6; this involves gently pressing the powder to create a smooth surface, effectively minimizing the unwanted background signals that often hinder accurate analysis in the low-angle region. The comparable background levels between the robotic arm-prepared samples and those prepared by skilled human operators confirm the effectiveness of the automated sample preparation technique in producing high-quality

samples suitable for a wide range of materials, including those with important structural features at low angles.

Table 1 lists the average anatase content and standard deviation for samples prepared by two human operators and the robotic arm. The results demonstrate the variability in the sample preparation between different human operators, as indicated by the differences in the average anatase content and standard deviation. Although the standard deviation of the robotic arm is slightly larger than that of the human operators, it is still sufficiently low; these results indicate that the automated sample preparation can achieve a level of consistency comparable to that of human operators. Thus, automated sample preparation has the potential to reduce human-induced variability.

The reliability and standardization potential of the robotic arm show the importance of integrating automated sample preparation with automated XRD measurements and data analysis for the future of material science research.

5.2 Optimizing the sample quantity for quantitative analysis

We investigated the effect of the sample quantity on the accuracy and precision of the quantitative XRD analysis by conducting an experiment to determine the minimum sample quantity needed to obtain the anatase content results with a standard deviation of less than 1% for the replicate measurements. A robotic arm was used to prepare samples with six different amounts (3.0, 5.0, 10.0, 20.0, 40.0, and 80.0 mg) of the TiO_2 mixture; this was the same mixture used in Section 5.1. For each sample quantity, the robotic arm was used to prepare five separate samples; this resulted in a total of 30 samples (6 quantities × 5 replicates). Fig. 4 shows the samples prepared by the robotic arm in different quantities.

Fig. 6 shows the XRD patterns of the different quantities of the TiO_2 samples (3 mg, 5 mg, 10 mg, 20 mg, 40 mg, and 80 mg) prepared by the robotic arm. Based on these patterns, although the peak intensities decrease as the sample quantity decreases, the overall shapes of the patterns are maintained, and the background intensities remain sufficiently low; these results show the consistency of the automated sample preparation method.

Fig. 7 shows the quantitative analysis results for the anatase content of the TiO_2 samples. Each data point is the average anatase content from the five samples at each sample quantity, and the error bars represent the standard deviation. The results indicate that as the sample quantity decreases, increased variability is observed in the estimated anatase content between the
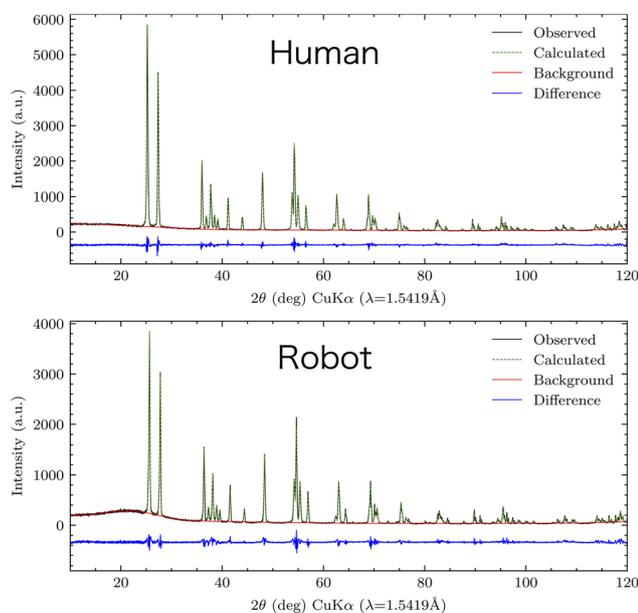

Fig. 5 Comparison of the XRD patterns and Rietveld refinement results for samples prepared by manual operation and the robotic arm (80 mg).

Table 1 Comparison of the sample preparation methods: manual operation and robotic arm. The standard deviation is abbreviated as SD in the table

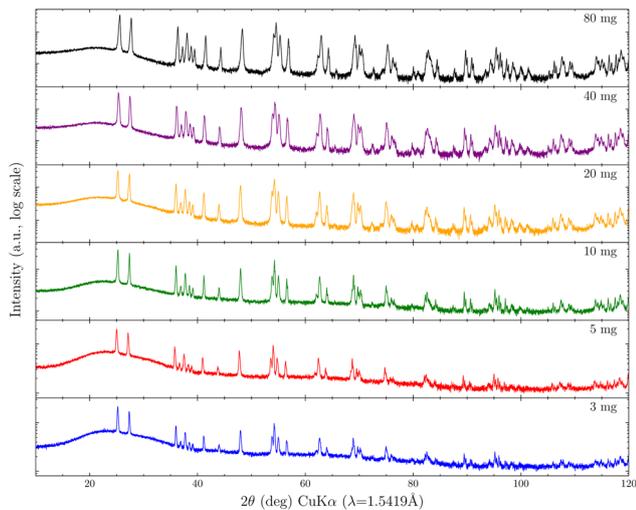| Method	Average anatase content (%)	SD (%)
Operator 1	52.4	0.4
Operator 2	52.2	0.1
Robotic arm	51.6	0.7

Fig. 6 XRD patterns from the different quantities of the TiO$_2$ samples (3 mg, 5 mg, 10 mg, 20 mg, 40 mg, and 80 mg) prepared by the robotic arm. The patterns are displayed on a logarithmic intensity scale.
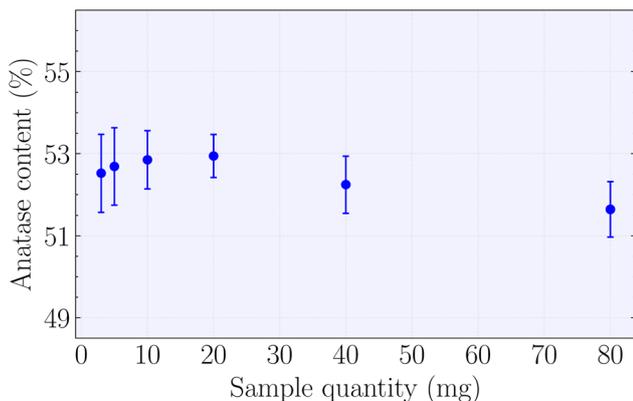

Fig. 7 Effect of sample quantity on the precision of quantitative XRD analysis. Average anatase content (%) with error bars representing the standard deviation for each sample quantity. The results show that the standard deviation increases as the sample quantity decreases, particularly for sample quantities of 5 mg or less. However, even at a minimum sample quantity of 3 mg, the standard deviation remains below 1%; thus, reliable quantitative results can be obtained using the automated sample preparation technique.

samples, as shown by the larger error bars. A slight increase in the average anatase content from the expected 51.4% was observed as the sample quantity decreased, rising from 51.6% for 80 mg samples to 52.5% for 3 mg samples. The standard deviation also changed, ranging from 0.5% to 0.7% for samples between 80 mg and 20 mg, and increasing to about 0.9% for samples of 10 mg or less.

These changes can be attributed to two main factors. First, the decrease in diffraction intensity as the sample quantity decreases. Analysis of the average maximum intensity of the diffraction patterns shows a reduction from about 2900 counts for 80 mg samples to about 1700 counts for 3 mg samples. This approximately 40% decrease in intensity directly affects the

statistical precision of the measurements. Second, the effect of sample inhomogeneity becomes more pronounced with smaller sample quantities, where local compositional variations can have a greater impact on the overall measurement results.

However, even at the minimum sample quantity of 3.0 mg, which is the lowest amount our system can prepare, the standard deviation of the anatase content was found to be 0.9%, indicating that quantitative results with the desired precision can be obtained. The systematic shift in the average values for smaller sample quantities warrants further investigation to determine whether it is due to the reduction in diffraction intensity, sample inhomogeneity, or other factors.

When proper sample preparation and analysis techniques are employed, reliable quantitative data can be obtained even with small sample quantities. This finding is significant considering that manual sample preparation typically involves using sample quantities of approximately 300 mg. Our system was able to automatically prepare the samples with sufficient accuracy and precision for the quantitative analysis using only 1% of the sample quantity traditionally used in manual preparation. By minimizing the sample quantity, the amount of material needed for synthesis can be reduced, potentially leading to shorter synthesis times and more efficient use of resources. As a result, high-throughput material characterization workflows can become more efficient, enabling the rapid analysis of a larger number of samples.

The optimization of the sample quantity, along with other key parameters, is essential for the development of efficient and reliable autonomous XRD systems for material discovery and optimization. Future research will focus on a more detailed investigation of the relationship between sample quantity and measurement precision, as well as optimization methods to obtain accurate results with small sample quantities. For example, extending measurement times to improve statistical precision or developing new sample preparation methods to enhance sample homogeneity could be considered.

5.3 Validation of the autonomous system with different mixture ratios

To further validate the effectiveness of the autonomous PXRD system, we prepared samples with different mixture ratios of anatase and rutile TiO$_2$ using the optimized sample quantity of 3 mg determined in Section 5.2. Two mixture ratios were tested: anatase : rutile = 9 : 1 and 7 : 3 by weight. For each mixture ratio, the robotic arm was used to prepare five samples 3 mg for each mixture; this resulted in a total of ten samples (2 ratios × 5 replicates).

Table 2 Quantitative analysis results for the anatase content in TiO$_2$ samples with different mixture ratios prepared by the autonomous system. The standard deviation is abbreviated as SD in the table

Mixture ratio (anatase : rutile)	Average anatase content (%)	SD (%)
9 : 1	89.8	1.1
7 : 3	70.9	0.7

Table 2 provides a summary of the quantitative analysis results for the anatase content in the TiO_2 samples with different mixture ratios. The average anatase contents for the 9 : 1 and 7 : 3 mixtures were found to be 89.8% and 70.9%, respectively. These values were in good agreement with the expected anatase content based on the prepared mixture ratios and demonstrated the accuracy of the autonomous system in quantifying the phase compositions. Moreover, the low standard deviations (1.1% for 9 : 1 and 0.7% for 7 : 3) of the anatase content for each mixture ratio highlight the high precision and reproducibility of the sample preparation and measurement processes performed by the autonomous system.

These results further validate the effectiveness of the autonomous PXRD system in accurately and precisely characterizing materials with different phase compositions, even when using small sample quantities. This capability is beneficial for high-throughput material discovery and optimization, where the ability to reliably analyze a large number of samples with varied compositions is essential.

5.4 Current limitations and future perspectives

The autonomous PXRD system developed in this study demonstrates progress in the automation of materials characterization. Here, we discuss the current limitations of the system and potential areas for future improvement.

5.4.1 Automation of sample preparation.
The current system requires manual intervention for weight-controlled sample loading, which may introduce potential variability and errors. While our robotic arm is capable of mixing reagents and filling powder samples into holders, it has not yet achieved sample weight control.

To address these limitations and achieve full automation, future research could focus on enhancing the automation capabilities in sample preparation. Specifically, the introduction of robotic weighing systems or automated dispensers is expected to enable precise and consistent control of sample quantities. We are also considering expanding the system's functionality to include reagent pre-preparation, particularly the weighing process.

Recent advances in robotic manipulation, such as the development of solid dispensing techniques using dual-arm robotic systems,[38] suggest the feasibility of automating complex tasks in materials research. Incorporating such technologies into our autonomous PXRD system may lead to more comprehensive automation of the materials research process.

5.4.2 Applicability to diverse samples.
While this study used TiO_2 as a typical sample, the optimal sample quantity may differ for other substances. Moreover, our method may face challenges when applied to materials with significantly different physical properties, particularly in terms of viscosity. It is important to note that materials which are difficult for human operators to handle, such as highly cohesive powders or those prone to static charging, may present similar or even greater challenges for automated systems. These challenges underscore the need for careful consideration of material properties in both manual and automated sample preparation processes.

Future research necessitates an examination of the system's applicability to a wider range of materials. This includes optimizing sample preparation protocols for materials with various physical properties. For instance, improvements in end-effector design or the development of new sample preparation techniques may be considered to accommodate materials with different characteristics, such as highly viscous materials or extremely light powders.

Additionally, evaluating the system's performance with multiphase systems and materials of complex composition presents an important challenge. Through these studies, we anticipate expanding the system's applicability and further enhancing the efficiency of high-throughput experiments in materials science.

5.4.3 Adaptability to different instruments.
The current system is optimized for a specific XRD instrument model. In particular, components such as the robotic arm's end-effector are designed to fit the equipment used in this study. Consequently, applying this system to different PXRD instruments would require modifying these parts to suit each specific device.

However, fundamental ideas such as the air cylinder mechanism for door operation and the automation of GUI operations using the PyAutoGUI library are considered applicable to various instruments. Future developments may explore the design of more flexible and adaptable systems based on these universal elements.

Specifically, adopting a modularized design approach and developing interfaces that can easily adapt to different instrument models could be considered. Additionally, the development of systems that utilize machine learning techniques to automatically learn the characteristics of new devices and optimize operational parameters is proposed as a future research direction.

These improvements may lead to the wider adoption of our autonomous PXRD system in various research environments and industrial applications. By enhancing adaptability to different instruments, it may contribute to the standardization and efficiency of materials research workflows, potentially accelerating the overall material development process.

6 Conclusion

In this study, we developed an autonomous robotic experimentation system for PXRD that combines the entire workflow from sample preparation to data analysis. Compared to traditional manual methods, our system provides improved efficiency, reproducibility, and reliability.

Our contributions include the following:

(1) We developed a system that integrates the entire workflow from sample preparation to data analysis, achieving high precision and reliability in sample preparation.

(2) We demonstrated the ability for the attainment of low-background patterns, particularly at low angles, which is essential for characterizing materials with important structural features in this region.

(3) We investigated the effect of the sample quantity on the accuracy and consistency of the quantitative analysis, minimized the amount of sample needed, and maintained reliable results. By reducing the needed sample quantity, our system enables high-throughput experimentation and more efficient use of resources.

(4) We validated the system with different mixture ratios and demonstrated its accuracy in quantifying the phase compositions; this is essential for high-throughput material discovery and optimization. The robustness of our system across different sample compositions highlights its adaptability and potential for application in a wide range of experiments and material systems.

While our system represents a significant advancement, it still has limitations. These include the need for manual sample loading and optimization for a specific XRD instrument model. Future work will focus on extending automation to include weighing and mixing of reagents, adapting the system to various PXRD instruments, and expanding its applicability to a wider range of materials. Additionally, we aim to enhance data analysis automation by integrating deep learning methods for initial model generation with our BBO-Rietveld refinement technique. By addressing these challenges, we aim to achieve a fully closed-loop material research process, potentially accelerating material discovery and optimization. However, expert oversight will remain crucial, especially for novel structures or complex materials. Our work lays the foundation for advanced autonomous systems in materials research, contributing to more efficient high-throughput experimentation in materials science.

Data availability

The data and code supporting the findings of this study are openly available. The Autonomous Robotic Experimentation (ARE) system for powder X-ray diffraction (PXRD) data is accessible at GitHub *via* [**https://github.com/quantumbeam/ARE-system-for-PXRD**], and the BBO-Rietveld analysis code is also available at GitHub *via* [**https://github.com/quantumbeam/BBO-Rietveld**]. Both repositories include detailed documentation and usage instructions to ensure reproducibility of the results. All information related to the Autonomous Robotic Experimentation (ARE) system for powder X-ray diffraction (PXRD) is included in the aforementioned repository and the ESI provided with this article.† The ESI† and additional data can be accessed through the Digital Discovery journal's online platform. By providing access to these datasets and code repositories, we aim to maintain high standards of transparency, research reproducibility, and to promote the reuse of our findings.

Author contributions

K. O. conceived the project. Y. Y. led the experimental work and the overall construction of the workflow. Y. N. also contributed to the construction of the workflow, automated the PXRD system and integrated the PXRD and BBO-Rietveld. R. T. assisted in the construction of the workflow. Y. T. was involved in the overall workflow design. All authors contributed to the writing of the paper.

Conflicts of interest

The authors declare no conflicts of interest.

References

1 D. P. Tabor, L. M. Roch, S. K. Saikin, C. Kreisbeck, D. Sheberla, J. H. Montoya, S. Dwaraknath, M. Aykol, C. Ortiz, H. Tribukait, C. Amador-Bedolla, C. J. Brabec, B. Maruyama, K. A. Persson and A. Aspuru-Guzik, *Nat. Rev. Mater.*, 2018, **3**, 5–20.

2 S. Steiner, J. Wolf, S. Glatzel, A. Andreou, J. M. Granda, G. Keenan, T. Hinkley, G. Aragon-Camarasa, P. J. Kitson, D. Angelone and L. Cronin, *Science*, 2019, **363**, eaav2211.

3 B. Burger, P. M. Maffettone, V. V. Gusev, C. M. Aitchison, Y. Bai, X. Wang, X. Li, B. M. Alston, B. Li, R. Clowes, N. Rankin, B. Harris, R. S. Sprick and A. I. Cooper, *Nature*, 2020, **583**, 237–241.

4 J. Li, J. Li, R. Liu, Y. Tu, Y. Li, J. Cheng, T. He and X. Zhu, *Nat. Commun.*, 2020, **11**, 2046.

5 B. P. MacLeod, F. G. L. Parlane, T. D. Morrissey, F. Häse, L. M. Roch, K. E. Dettelbach, R. Moreira, L. P. E. Yunker, M. B. Rooney, J. R. Deeth, V. Lai, G. J. Ng, H. Situ, R. H. Zhang, M. S. Elliott, T. H. Haley, D. J. Dvorak, A. Aspuru-Guzik, J. E. Hein and C. P. Berlinguette, *Sci. Adv.*, 2020, **6**, eaaz8867.

6 M. B. Rooney, B. P. MacLeod, R. Oldford, Z. J. Thompson, K. L. White, J. Tungjunyatham, B. J. Stankiewicz and C. P. Berlinguette, *Digital Discovery*, 2022, **1**, 382–389.

7 B. Zhang, L. Merker, A. Sanin and H. S. Stein, *Digital Discovery*, 2022, **1**, 755–762.

8 B. P. MacLeod, F. G. L. Parlane, A. K. Brown, J. E. Hein and C. P. Berlinguette, *Nat. Mater.*, 2022, **21**, 722–726.

9 H. Fakhruldeen, G. Pizzuto, J. Glowacki and A. I. Cooper, *2022 International Conference on Robotics and Automation (ICRA)*, 2022, pp. 6013–6019.

10 N. J. Szymanski, B. Rendy, Y. Fei, R. E. Kumar, T. He, D. Milsted, M. J. McDermott, M. Gallant, E. D. Cubuk, A. Merchant, H. Kim, A. Jain, C. J. Bartel, K. Persson, Y. Zeng and G. Ceder, *Nature*, 2023, **624**, 86–91.

11 Z. Ren, Z. Ren, Z. Zhang, T. Buonassisi and J. Li, *Nat. Rev. Mater.*, 2023, **8**, 563–564.

12 J. Chen, S. R. Cross, L. J. Miara, J.-J. Cho, Y. Wang and W. Sun, *Nat. Synth.*, 2024, **3**, 606–614.

13 C. Baerlocher, T. Weber, L. McCusker, L. Palatinus and S. Zones, *Science*, 2011, **333**, 1134–1137.

14 P. Cui, D. P. McMahon, P. R. Spackman, B. M. Alston, M. A. Little, G. M. Day and A. I. Cooper, *Chem. Sci.*, 2019, **10**, 9988–9997.

15 C. Gropp, T. Ma, N. Hanikel and O. Yaghi, *Science*, 2020, **370**, eabd6406.

16 A. A. Bunaciu, E. Udriștioiu and H. Aboul-Enein, *Crit. Rev. Anal. Chem.*, 2015, **45**, 289–299.

17 A. L. Grzesiak, M. Lang, K. Kim and A. J. Matzger, *J. Pharm. Sci.*, 2003, **92**, 2260–2271.

18 N. Chieng, T. Rades and J. Aaltonen, *J. Pharm. Biomed. Anal.*, 2011, **55**, 618–644.

19 J. Li, S. A. Bourne and M. R. Caira, *Chem. Commun.*, 2011, **47**, 1530–1532.

20 M. D. Eddleston, S. Sivachelvam and W. Jones, *CrystEngComm*, 2013, **15**, 175–181.

21 X. Yao, R. F. Henry and G. G. Z. Zhang, *J. Pharm. Sci.*, 2023, **112**, 237–242.

22 A. M. Lunt, H. Fakhruldeen, G. Pizzuto, L. Longley, A. White, N. Rankin, R. Clowes, B. Alston, L. Gigli, G. M. Day, A. I. Cooper and S. Y. Chong, *Chem. Sci.*, 2024, **15**, 2456–2463.

23 H. Ito, M. Muromoto, S. Kurenuma, S. Ishizaka, N. Kitamura, H. Sato and T. Seki, *Nat. Commun.*, 2013, **4**, 2009.

24 D. Chen, J. Zhao, P. Zhang and S. Dai, *Polyhedron*, 2019, **162**, 59–64.

25 F. Palazon, Y. El Ajjouri, P. Sebastia-Luna, S. Lauciello, L. Manna and H. J. Bolink, *J. Mater. Chem. C*, 2019, **7**, 11406–11410.

26 Z. Li, M. A. Najeeb, L. Alves, A. Z. Sherman, V. Shekar, P. Cruz Parrilla, I. M. Pendleton, W. Wang, P. W. Nega, M. Zeller, J. Schrier, A. J. Norquist and E. M. Chan, *Chem. Mater.*, 2020, **32**, 5650–5663.

27 G. I. Lampronti, A. A. L. Michalchuk, P. P. Mazzeo, A. M. Belenguer, J. K. M. Sanders, A. Bacchi and F. Emmerling, *Nat. Commun.*, 2021, **12**, 6134.

28 K.-Y. Baek, W. Lee, J. Lee, J. Kim, H. Ahn, J. I. Kim, J. Kim, H. Lim, J. Shin, Y.-J. Ko, H.-D. Lee, R. H. Friend, T.-W. Lee, J. Lee, K. Kang and T. Lee, *Nat. Commun.*, 2022, **13**, 4263.

29 Ö. Almarsson, M. B. Hickey, M. L. Peterson, S. L. Morissette, S. Soukasene, C. McNulty, M. Tawa, J. M. MacPhee and J. F. Remenar, *Cryst. Growth Des.*, 2003, **3**, 927–933.

30 T. A. Stegk, R. Janssen and G. A. Schneider, *J. Comb. Chem.*, 2008, **10**, 274–279.

31 U. Eckstein, M. Kuhfuß, T. Fey and K. G. Webber, *Adv. Eng. Mater.*, 2024, 2302126.

32 Y. Nakajima, M. Hamaya, Y. Suzuki, T. Hawai, F. v. Drigalski, K. Tanaka, Y. Ushiku and K. Ono, *2022 IEEE/RSJ International Conference on Intelligent Robots and Systems (IROS)*, 2022, pp. 2320–2326.

33 Y. Nakajima, M. Hamaya, K. Tanaka, T. Hawai, F. von Drigalski, Y. Takeichi, Y. Ushiku and K. Ono, *2023 IEEE/RSJ International Conference on Intelligent Robots and Systems (IROS)*, 2023, pp. 8283–8290.

34 Y. Ozaki, Y. Suzuki, T. Hawai, K. Saito, M. Onishi and K. Ono, *npj Comput. Mater.*, 2020, **6**, 75.

35 B. H. Toby and R. B. Von Dreele, *J. Appl. Crystallogr.*, 2013, **46**, 544–549.

36 T. Akiba, S. Sano, T. Yanase, T. Ohta and M. Koyama, *Proceedings of the 25th ACM SIGKDD International Conference on Knowledge Discovery and Data Mining*, 2019, pp. 2623–2631.

37 G. Guo, J. Goldfeder, L. Lan, A. Ray, A. H. Yang, B. Chen, S. J. L. Billinge and H. Lipson, *npj Comput. Mater.*, 2024, **10**, 209.

38 Y. Jiang, H. Fakhruldeen, G. Pizzuto, L. Longley, A. He, T. Dai, R. Clowes, N. Rankin and A. I. Cooper, *Digital Discovery*, 2023, **2**, 1733–1744.